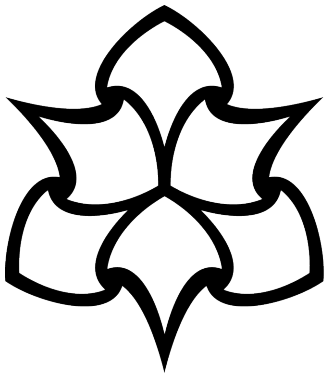

Waste peat ash mineralogy and transformation to microporous zeolites

Ifeoma V. Joseph, Giulia Roncaglia, Lubomira Tosheva, Aidan M. Doyle*

Department of Natural Sciences, Manchester Metropolitan University, Chester St., Manchester, M1 5GD, United Kingdom.

* Corresponding author: a.m.doyle@mmu.ac.uk

Abstract

The combustion of peat fuel for industrial scale power generation and domestic heating produces toxic ash, most of which is presently buried in landfill. In this study, the mineralogy of waste peat ash was determined, followed by its successful use as a starting reagent to prepare zeolites. X-ray diffraction (XRD) confirmed the presence of quartz, anhydrite, calcite, lime, merwinite and magnetite in peat ash, and that a single extraction step using mineral acid was sufficient to remove all non-quartz crystal phases. Alkali fusion of the acid-extracted samples produced GIS-type zeolite. LTA- and FAU-type were also prepared by altering the Si/Al ratio and extending the ageing time. Experiments confirmed that the LTA- and FAU-type zeolites were active in the simultaneous adsorption of lead, cadmium, cobalt, zinc and copper from aqueous solutions, with similar quantities of metals removed to those using a reference zeolite.

Keywords; Peat ash utilisation; zeolite; pyrolysis; waste management; water purification.

1. Introduction

Peat is a carbon based material produced from partially decayed vegetation that builds up over a duration typically up to approximately 12,000 years [1,2]. The deficiencies of oxygen and nutrients in waterlogged bogs and fens (peatlands) limit the decay rate of vegetation such that there is an accumulation of peat over time. These peatlands cover an estimated global area of 4m km^2, which equates to 2-3% of the total land area, and are found mainly in Russia, North and South America, Northern Europe and South-East Asia, including lower quantities in locations such as central Africa [1,2]. Peat is classified as an intermediate fuel i.e. between biomass and fossil fuel (lignite). Total global consumption is estimated at 17m tons per annum, over 99% of which is used in Northern Europe for the production of heat and electricity [3]. Ireland is the largest user, consuming 3.8m tons annually from peatlands that cover approximately 20% of the national land area [4]. Most of this is used in thermal power plants to generate 8.5% of Ireland's electricity [5,6]. While renewable fuel sources are increasingly being used as a substitute for peat (at least partially in the short term), the production of electricity in Ireland using peat based fuel is an established industry with a secure, indigenous energy source, and will, therefore, continue for the foreseeable future.

Peat ash is the main waste product of combustion at thermal power stations, some of which is disposed of by landfill burial. The alkalinity of peat ash alters the soil quality of the landfill site such that only alkali tolerant plants can grow during the years immediately after disposal. The composition of peat ash varies with location but typically contains a mixture of silicon-, aluminium-, calcium- and iron-containing species, and a range of toxic elements including arsenic and cadmium [7-10]. While its elemental composition has been well studied, a definitive characterisation of peat ash mineralogy is lacking in the literature. The few papers that discuss peat ash infer crystal phases from (a) elemental composition by scanning electron microscopy/energy-dispersive X-ray spectroscopy (SEM/EDAX) or X-ray fluorescence (XRF)

only and/or (b) unseen XRD data; the reader is thus advised to treat such assertions with caution. For example, quartz, microcline, albite and calcium sulfate were reported to be present in peat ash samples, although no XRD results were shown [7, 8].

The transformation of peat ash to a useful value-added product with industrial applications would be a significant improvement on the current method of disposal. One such possibility is to use peat ash to prepare zeolites, which are high surface area aluminosilicates widely used for water treatment and purification, humidity control, and heterogeneous catalysis [11]. The combustion of fossil fuels and biomass produces ash residue that contains silicon and aluminium based minerals in appropriate quantities to those used to prepare aluminosilicate zeolites. Coal fly ash has been extensively studied as a zeolite synthesis reagent, and a variety of zeolite architectures were successfully prepared using the alkali fusion method [12-23]. More recently, there are reports showing zeolite preparation using ash from the following renewable biomass sources: rice husk [24-27] eucalyptus bark residue [28], pulp from paper industry [29], sawdust and pine bark [30], bamboo [31] and cogon grass [32].

We now report the mineralogy of peat ash and its successful transformation to pure zeolite using a single stage purification step. To our knowledge, this is the first report of zeolite prepared using peat ash. The zeolites formed removed heavy metals from aqueous solution with practically similar quantities to those of a reference zeolite.

2. Materials and Methods

2.1 Materials

Peat ash, from Ireland, was collected and combusted as follows: (a) sample A (lime added), *Bord na Móna ltd.*, industrial boiler (b) sample B, air-dried peat sods from county Roscommon, domestic stove. The following is a list of the materials' source/supplier and purity; hydrochloric acid (HCl), concentration >37%, Fluka; nitric acid 70% w/w; sodium hydroxide (NaOH)

pellets (anhydrous), extra pure, Sigma-Aldrich; sodium aluminate ($NaAlO_2$), general purpose, Fischer; sodium silicate solution, general purpose, Merck. Copper(II) nitrate trihydrate $Cu(NO_3)_2.3H_2O$, cobalt(II) nitrate hexahydrate $Co(NO_3)_2.6H_2O$, lead nitrate $Pb(NO_3)_2$, zinc nitrate hexahydrate $Zn(NO_3)_2.6H_2O$ and cadmium nitrate tetrahydrate $Cd(NO_3)_2.4H_2O$ were all 99.99% purity and supplied by Sigma-Aldrich.

2.2 Zeolite synthesis

The samples were calcined in air at 600 °C (sample A) and 800 °C (sample B) for 4 h to remove organic matter. Acid extraction was conducted by treating 30 g of calcined peat ash in 500 cm^3 acid for 5 h as follows: Sample A was stirred in 5 M HNO_3 at room temperature, and sample B was refluxed in 5 M HCl at 95 °C. The product was recovered by filtration and dried at 80 °C. Unless otherwise stated, 1 part of the acid extracted ash was ground in a mortar and pestle with 2.4 parts (by mass) NaOH, heated at 600 °C in air for 3 h in a furnace, and crushed to powder form after cooling to ambient temperature. 1 part alkali fused ash was then added to 10 parts water in a polypropylene bottle, stirred at room temperature for 3 days, and hydrothermally treated at 90 °C for 24 h. Sodium aluminate was added prior to alkali fusion to give Si/Al ratios (of synthesis reagents) of 5 and 1 to produce GIS and LTA, respectively. Additional ageing of the Si/Al ratio 1 suspension was done for 4 days at 35 °C to produce FAU. Products were recovered by filtration and calcined in air at 550 ºC for 4 h using a ramp rate of 5 °C min^{-1}. A reference FAU zeolite was prepared from a synthesis solution with the molar composition $8NaOH : 0.2Al_2O_3 : 1.0SiO_2 : 200H_2O$ [33]. The hydrothermal treatment was performed at 80 °C for 24 h.

2.3 Characterisation

XRD was conducted in ambient conditions using a Panalytical X'Pert Powder diffractometer with Cu Kα radiation (λ = 1.5406 Å). All powder diffraction patterns were recorded from 4 to 120° 2θ with step size 0.013 ° and step time 50 s, using an X-ray tube operated at 40 kV and 30 mA with fixed ¼ ° anti-scatter slit. A Rigaku NEX-CG (XRF) spectrometer was used for elemental analysis using the loose powder method under vacuum. Nitrogen adsorption/desorption measurements were carried out using a Micromeritics ASAP 2020 surface area analyser at -196 °C. Samples were degassed under vacuum ($p < 10^{-5}$ mbar) for 5 h at 200 °C prior to analysis. Brunauer–Emmett–Teller (BET) surface areas of the samples were calculated in the relative pressure range 0.05-0.30. Microscopic images were recorded using a JEOL JSM-5600LV SEM.

2.4 Adsorption study

$Cu(NO_3)_2.3H_2O$, $Co(NO_3)_2.6H_2O$, $Pb(NO_3)_2$, $Zn(NO_3)_2.6H_2O$ and $Cd(NO_3)_2.4H_2O$ were dissolved together in water and diluted to give a solution that was 100 ppm in each of Cu, Co, Pd, Zn and Cd. 20 cm^3 of this solution were added to 0.1 g LTA (sample A), stirred at 180 rpm for 1 h at room temperature and the solid removed by filtration**.** The concentrations of metals before and after adsorption were determined using a Thermo Scientific iCAP 6000 Series inductively coupled plasma-optical emissions spectrometer (ICP-OES).

3. Results and Discussion

3.1 Crystallography and elemental composition

SEM images, Fig. 1, show that both raw and calcined peat ash lack any regular morphology, which is in contrast to the spherically shaped particles routinely observed for coal fly ash [12]. Results also showed that calcination did not cause an observable transformation in particle morphology. Phase identification, performed by matching the XRD peak positions in Fig. 2

against the Crystallography Open Database, confirms that the major phases detected for sample A are anhydrite ($CaSO_4$), quartz (SiO_2), calcite ($CaCO_3$), lime (CaO) and merwinite ($Ca_3Mg(SiO_4)_2$). Sample B contains anhydrite, quartz and magnetite (Fe_3O_4). A quantitative elemental analysis using XRF, Table 1, shows the 10 most concentrated elements present (for sample A) and confirms that the major 'impurities' (in terms of zeolite synthesis) are Ca and Fe based species. The major element present in Sample A is Ca at 53.9 wt% (as oxide) in agreement with the XRD analysis (Fig. 2). Sample B contains 21.2 wt% CaO and 22.0 wt% Fe_2O_3. The greater quantity of CaO in sample A is due to the addition of lime to commercial peat to reduce SO_x emissions, which may have reacted to produce anhydrite. It is interesting then that sample B, which has not been treated with lime, also contains anhydrite.

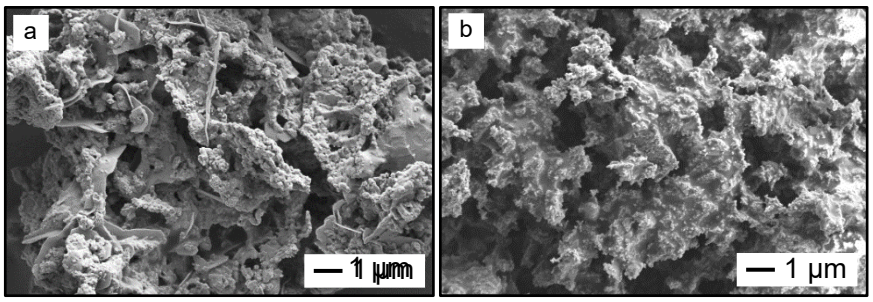

Fig. 1. Typical SEM images of peat ash: (a) raw and (b) calcined.

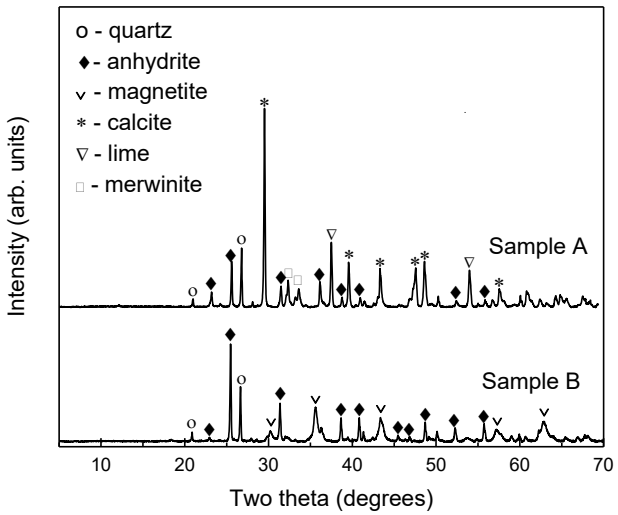

Fig. 2. XRD powder patterns of calcined peat ash.

143

144 It is not possible to make a meaningful comparison of the XRD results presented here with
145 published data on peat ash mineralogy, as such reports contain insufficient results [7,8].
146 However, all such studies confirm that the main elements present in peat ash are Ca, Fe, Si and
147 Al, which correlates well with our XRD and XRF results.

148

149 Table 1: XRF elemental composition of peat ash in wt% following calcination and acid extraction.

	A		B	
	Calcined	**Acid extracted**	**Calcined**	**Acid extracted**
CaO	53.9	0.81	21.2	0.77
SiO_2	9.47	71.4	12.7	76.9
SO_3	7.32	0.58	22.4	0.26
Fe_2O_3	4.81	1.29	22.0	0.61
MgO	2.20	0.12	10.4	0.35
Al_2O_3	1.63	2.55	6.58	3.77
MnO	0.35	0.03	0.30	0.02
P_2O_5	0.26	0.05	1.87	0.05
K_2O	0.19	0.97	0.97	1.12
TiO_2	0.15	0.50	0.45	0.90

150

151 Dissolution by acid extraction considerably reduced the quantities of Ca and Fe in both
152 samples. The Si/Al ratios of acid extracted peat ashes are 28.0 for sample A and 20.4 for sample
153 B. XRD patterns confirm that acid extraction removes all detectable non-quartz crystalline
154 phases, Fig. 3. The majority of zeolite preparations using coal ash do not remove impurities by
155 acid extraction, so it is not surprising that a greater ratio of NaOH to ash is required for the peat
156 ash samples explored here to achieve full quartz decomposition due to the higher quantity of
157 quartz [12]. Fig. 3 shows that the mass ratio of 1.2:1 NaOH to ash (chosen as a starting point
158 based on reference [22]) was insufficient but that higher ratios removed quartz completely; a
159 mass ratio of 2.4:1 was used in all further preparations. The other peaks in Fig. 3 confirm the
160 presence of silicates and aluminosilicates, as reported in the literature [34].

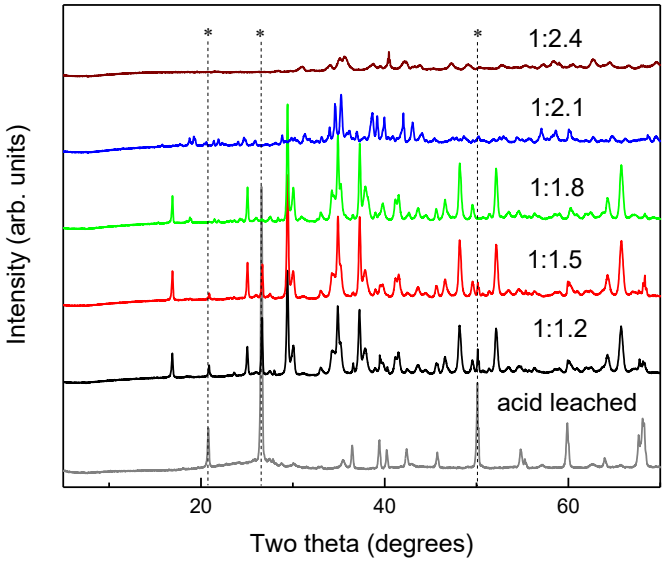

Fig. 3. XRD patterns of sample A after acid leaching and the acid-leached sample after alkali fusion at 600 °C using different sample:NaOH mass ratios as indicated on the figure; the asterisks indicate quartz peaks.

3.2 Zeolite formation

The XRD patterns in Figs. 4 and 5 confirm that peat ash was transformed to zeolite frameworks GIS, LTA and FAU through changes in the synthesis parameters viz. addition of sodium aluminate for LTA, and extended ageing time for FAU. Non-zeolitic crystalline phases were not observed by XRD in any detectable quantities. The effect of altering the Si/Al ratio by adding external silica was found to alter the crystal phase produced in a study of the crystallisation mechanism of zeolite from coal fly ash, where FAU was not formed until the Si/Al ratio was reduced to approximately 1.5 [35]. SEM images, Fig. 6, show the morphology of GIS, the characteristic cubic ca. 1 μm sized particles of LTA and the sub-micron agglomerated FAU particle morphology, providing further evidence of the presence of these phases. The Si/Al ratios are shown in Table 2: the Si/Al ratios of FAU are 1.32 and 1.35, so these samples are zeolite X. The highest BET surface areas were recorded for the FAU structures, which were calculated to be 486 and 319 $m^2 g^{-1}$.

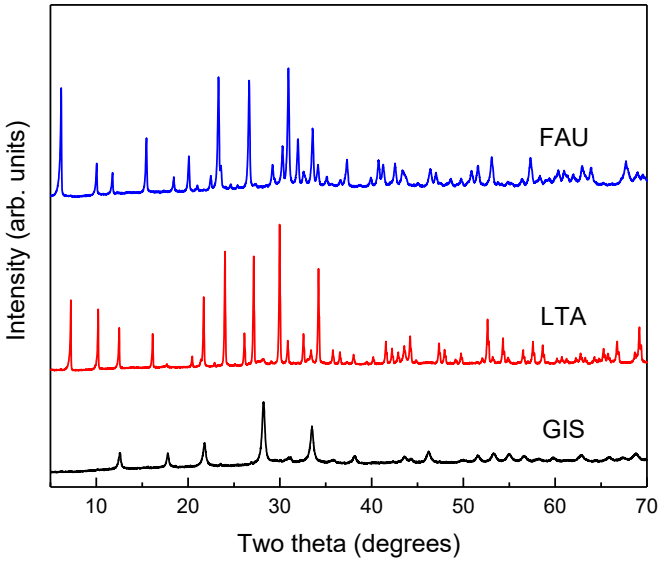

Fig. 4 XRD patterns of zeolites prepared using sample A.

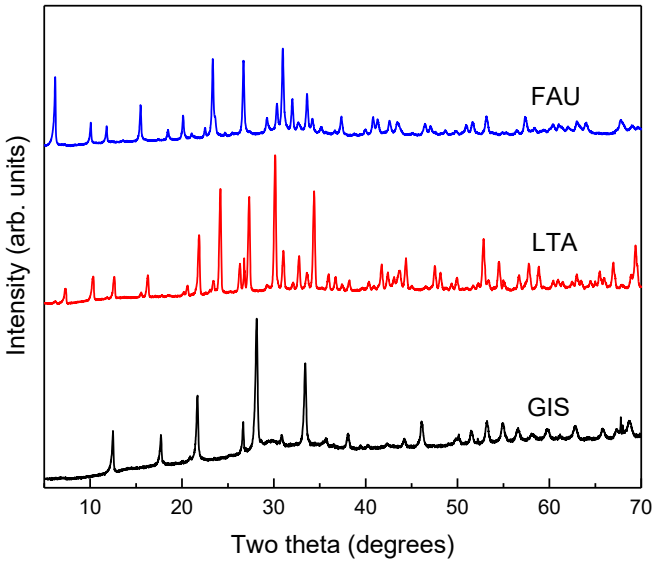

Fig. 5 XRD patterns of zeolites prepared using sample B.

188 Table 2: BET surface areas and Si/Al elemental ratios.

	Surface area (m^2 g^{-1})		Si/Al	
	A	**B**	**A**	**B**
Raw	24	25	4.04	1.55
Calcined	6	22	4.94	1.64
FAU	486	319	1.32	1.35
LTA	84	55	1.41	1.35
GIS	77	104	2.83	2.83

189

190

191

192

193

194

195

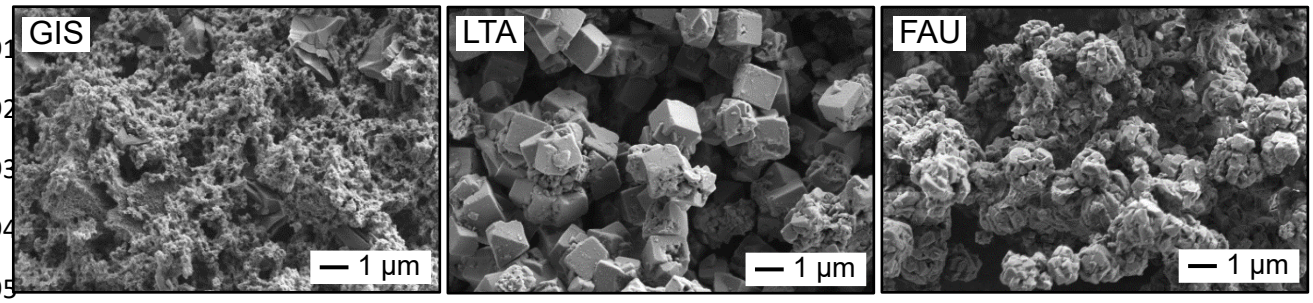

196 Fig. 6. Typical SEM images of different zeolites types prepared from peat ash.

197

198 The characteristics of zeolites prepared from peat ash also compare well with analogous studies
199 using fly ash. For example, the highest surface area reported by Tosheva et al. for FAU
200 prepared from fly ash was 441 m^2 g^{-1}, relative to 486 m^2 g^{-1} for that prepared here [23]. The
201 classification of coal is based on the relative amounts of organic and inorganic materials, age,
202 and quantity of heat energy that can be produced. Most reports in the literature describing coal
203 ash to zeolite conversions are for sub-bituminous (up to 45% carbon) bituminous (86%) and
204 anthracitic (97%) coal types. Lignite has lower carbon content than sub-bituminous coal and,
205 because it is formed over time from compressed peat, which has carbon content less than 40-
206 55%, seems the most appropriate comparison to the results presented here [1-3]. Kunecki et al.
207 used lignite, containing quartz, anhydrite and gehlenite, to prepare zeolite [36]. Both LTA and
208 FAU frameworks were prepared by varying experimental conditions, but not in pure form. The
209 highest BET surface area for FAU was 256 m^2 g^{-1}, which was significantly lower than the FAU

from either sample in this study, 486 and 319 m^2 g^{-1}. The increased crystal purity and surface area for zeolite prepared using peat ash is tentatively attributed to the removal of impurities in the starting material by acid extraction. Anhydrite is highly soluble in aqueous solution and its presence during zeolite crystallisation, as in the case of lignite to zeolite, reduces the solubility of silicates and aluminosilicates, which will negatively impact both the formation of zeolite nuclei and the subsequent dissolution and crystallisation of zeolite during hydrothermal treatment. Furthermore, ions in solution are known to interact with zeolite frameworks during crystallisation, so the Ca^{2+} and SO_4^{2-} ions from anhydrite may have a negative effect on the formation of zeolite [37].

3.3 Adsorption study

The prepared zeolites were tested as adsorbents in the removal of heavy metals lead, cadmium, cobalt, zinc and copper from aqueous solution; these metals were chosen on the basis of their toxicity and presence in wastewater streams [38]. The results, Fig. 7, showed that all zeolites actively removed the range of metals between 10 and 60 minutes, in which the quantities of lead, cadmium, zinc and copper adsorbed using peat ash prepared zeolites were slightly higher than those measured for the FAU- reference. In the case of cobalt, adsorption was higher using FAU-type zeolites than LTA-, while the most active adsorbent was that prepared from sample A, which showed near identical properties to that of the reference zeolite. A more in-depth study of metals adsorption on zeolites viz. influence of concentration, temperature, and kinetics is currently underway and will be published as a follow up to this paper. While the focus of this paper is the preparation of pure zeolite from peat ash, the adsorption results are included to validate the efficacy of such materials in real applications.

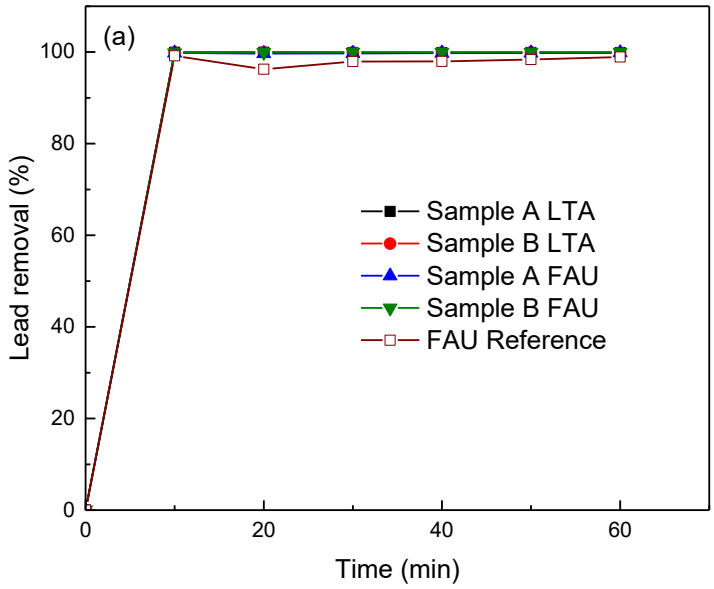
(a)
Lead removal (%)
Time (min)
Sample A LTA
Sample B LTA
Sample A FAU
Sample B FAU
FAU Reference

233

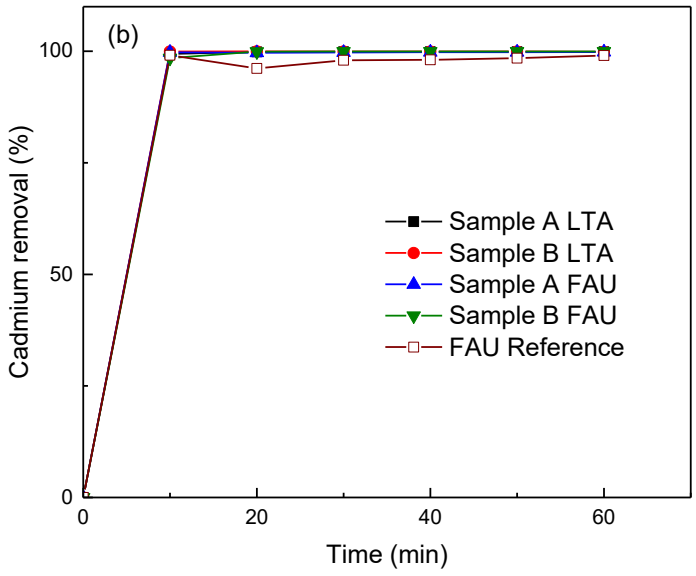
(b)
Cadmium removal (%)
Time (min)
Sample A LTA
Sample B LTA
Sample A FAU
Sample B FAU
FAU Reference

234

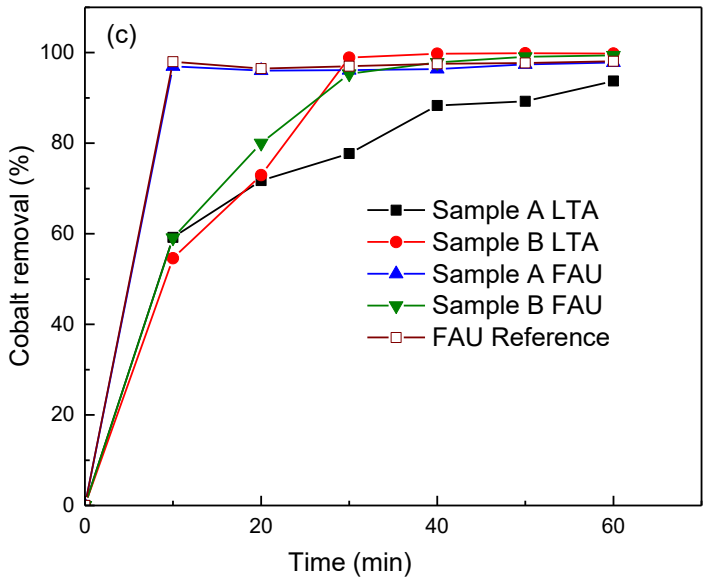
(c)
Cobalt removal (%)
Time (min)
Sample A LTA
Sample B LTA
Sample A FAU
Sample B FAU
FAU Reference

235

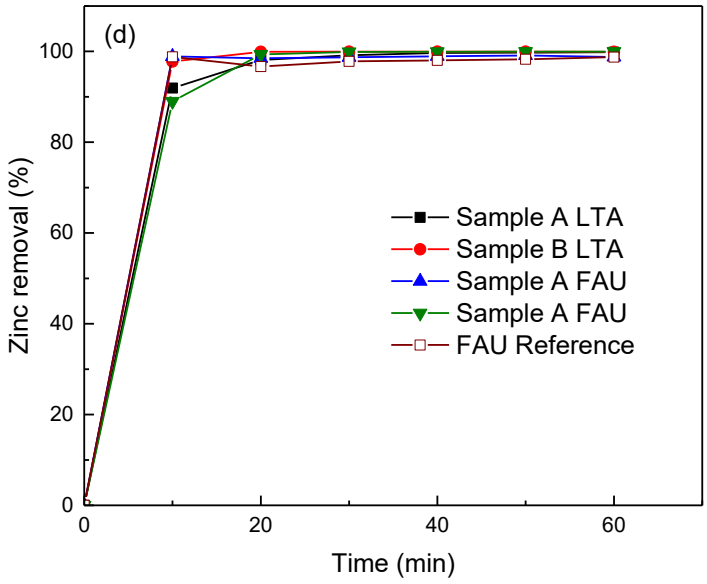
(d)
Zinc removal (%)
Time (min)
Sample A LTA
Sample B LTA
Sample A FAU
Sample A FAU
FAU Reference

236

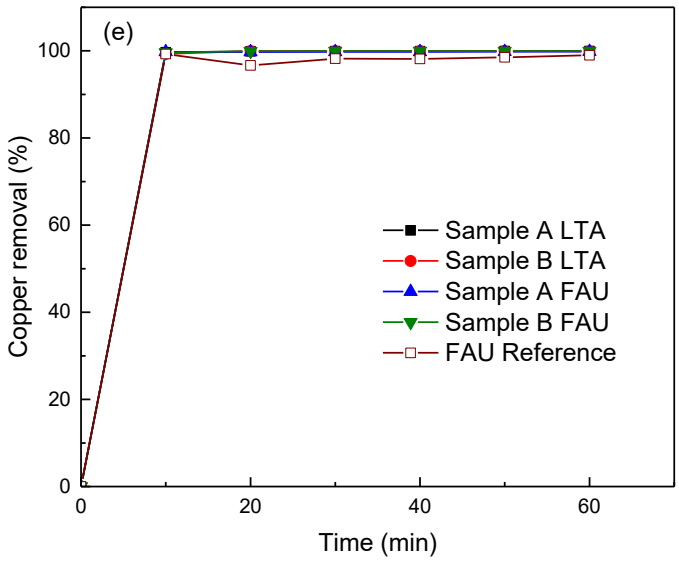

Fig. 7. Metal removal (as % of original concentration) of (a) lead (b) cadmium (c) cobalt (d) zinc and (e) copper on LTA- and FAU-type zeolites prepared from peat ash and an FAU- reference.

4. Conclusions

Zeolites were successfully prepared from peat ash using a combination of acid leaching, alkali fusion and hydrothermal treatment. The framework structure was systematically varied such that crystal phases of GIS, LTA and FAU-type zeolites were each prepared. The prepared zeolites were active in the removal of a range of metals from aqueous solution.

Acknowledgments:

The authors thank; Patrick Bowens, Co. Roscommon, and Imelda Egan and Colman Hynes, Bord na Móna, for supplying peat ash; Dr Paul Bolger, University College Cork, for arranging the link with Bord na Móna. Ifeoma V Joseph is grateful to the Schlumberger Foundation for funding a PhD studentship; Giulia Roncaglia is grateful to Erasmus+ and Manchester Metropolitan University for financial assistance.

255 **References**

256 1. F. Parish, A.A. Sirin, D. Charman, H. Joosten, T. Minayeva, M. Silvius, Assessment on
257 Peatlands, Biodiversity and Climate Change: Executive Summary. Global Environmental
258 Centre, Malaysia and Wetlands International, Wageningen, The Netherlands, 2007.
259 2. E. Lappalainen, Global Peat Resources, The International Peat Society, Finland 1996.
260 3. World Energy Council Report, World Energy Resources 2013 Survey: Peat.
261 4. Department of Agriculture, Food and the Marine Ireland, Rural Development Programme
262 2014a.
263 5. Sustainable Energy Authority of Ireland 2017 Report, Energy in Ireland 1990-2016.
264 6. Eirgrid Group, All-Island Generation Capacity Statement 2017-2026.
265 7. J. Fagerström, I.-L. Näzelius, C. Gilbe, D. Boström, M. Öhman, C. Boman, Influence of peat
266 ash composition on particle emissions and slag formation in biomass grate co-combustion,
267 Energy Fuels 28 (2014) 3403-3411. https://dx.doi.org/10.1021/ef4023543.
268 8. L. Pommer, M. Öhman, D. Boström, J. Burvall, R. Backman, I. Olofsson, A. Nordin,
269 Mechanisms behind the positive effects on bed agglomeration and deposit formation
270 combusting forest residue with peat additives in fluidized beds, Energy Fuels 23 (2009) 4245-
271 4253. https://doi.org/10.1021/ef900146e.
272 9. B-M. Steenari, O. Lindqvist, Fly ash characteristics in co-combustion of wood with coal, oil
273 or peat, Fuel 78 (1999) 479-488. https://doi.org/10.1016/S0016-2361(98)00177-X.
274 10. S.V. Vassilev, D. Baxter, L.K. Andersen, C.G. Vassileva, An overview of the composition
275 and application of biomass ash. Part 1. Phase–mineral and chemical composition and
276 classification, Fuel 10 (2013) 40-76. https://doi.org/10.1016/j.fuel.2012.09.041.
277 11. J. Weitkamp, Zeolites and catalysis, Solid State Ionics 131 (2000) 175-188.
278 https://doi.org/10.1016/S0167-2738(00)00632-9.
279 12. C. Belviso, State-of-the-art applications of fly ash from coal and biomass: A focus on
280 zeolite synthesis processes and issues, Prog. Energy Combust. Sci. 65 (2018) 109-135.
281 https://doi.org/10.1016/j.pecs.2017.10.004.
282 13. X. Querol, N. Moreno, J.C. Umaña, A. Alastuey, E. Hernández, A. López-Soler, F. Plana,
283 Synthesis of zeolites from coal fly ash: an overview. Int. J. Coal Geol. 50 (2002) 413-423.
284 https://doi.org/10.1016/S0166-5162(02)00124-6.
285 14. X. Querol, J.C. Umaña, F. Plana, A. Alastuey, A. López-Soler, A. Medinaceli, A. Valero,
286 M.J. Domingo, E. Garcia-Rojo. Synthesis of Na zeolites from fly ash in a pilot plant
287 scale. Examples of potential environmental applications, Fuel 80 (2001) 857-865.

15. N. Murayama H. Yamamoto J. Shibata, Mechanism of zeolite synthesis from coal fly ash by alkali hydrothermal reaction. Int. J. Miner. Process. 64 (2002) 1-17. https://doi.org/10.1016/S0301-7516(01)00046-1.

16. H. Tanaka, S. Matsumura, R. Hino, Formation process of Na-X zeolites from coal fly ash. J. Mater. Sci. 39 (2004) 1677-1682. https://doi.org/10.1023/B:JMSC.0000016169.85449.86.

17. T.T. Wałek, F. Saito, Q. Zhang, The effect of low solid/liquid ratio on hydrothermal synthesis of zeolites from fly ash. Fuel 87 (2008) 3194-3199. https://doi.org/10.1016/j.fuel.2008.06.006.

18. H. Tanaka, A. Fujii. Effect of stirring on the dissolution of coal fly ash and synthesis of pure-form Na-A and -X zeolites by two-step process, Adv. Powder Technol. 20 (2009) 473-479. https://10.1016/j.apt.2009.05.004

19. M. Gross-Lorgouilloux, P. Gaullet, M. Soulard, J. Patarin, E. Moleiro, I. Saude, Conversion of coal fly ashes into faujasite under soft temperature and pressure conditions. Mechanisms of crystallisation, Microporous Mesoporous Mater. 131 (2010) 407-417. https://doi.org/10.1016/j.micromeso.2010.01.022.

20. N. Shigemoto, H. Hayashi, K. Miyaura, Selective formation of Na-X zeolite from coal fly ash by fusion with sodium hydroxide prior to hydrothermal reaction, J. Mater. Sci. 28 (1992) 4781-4786. https://doi.org/10.1007/BF00414272.

21. H.-L. Chang, W.-H. Shih, A general method for the conversion of fly ash into zeolites as ion exchangers for cesium, Ind. Eng. Chem. Res. 37 (1998) 71-78. https://10.1021/ie970362o.

22. A. Molina, C. Poole, A comparative study using two methods to produce zeolites from fly ash, Miner. Eng. 17 (2004) 167-173. https://doi.org/10.1016/j.mineng.2003.10.025.

23. L. Tosheva, A. Brockbank, B. Mihailova, J. Sutula, J. Ludwig, H. Potgieter, J. Verran, Micron- and nanosized FAU-type zeolites from fly ash for antibacterial applications, J. Mater. Chem. 22 (2012) 16897-16905. https://10.1039/C2JM33180B.

24. D. Prasetyoko, Z. Ramli, S. Endud, H. Hamdan, B. Sulikowski, Conversion of rice husk ash to zeolite beta, Waste Management, 26 (2006) 1173-1179. https://doi.org/10.1016/j.wasman.2005.09.009.

25. R.K. Vempati, R. Borade, R.S. Hegde, S. Komarneni, Template free ZSM-5 from siliceous rice hull ash with varying C contents, Microporous Mesoporous Mater. 93 (2006) 134-140. https://doi.org/10.1016/j.micromeso.2006.02.008.

26. E.-P. Ng, H. Awala, K.-H. Tan, F. Adam, R.d Retoux, S. Mintova, EMT-type zeolite nanocrystals synthesized from rice husk, Microporous Mesoporous Mater. 204 (2015) 204-209. https://doi.org/10.1016/j.micromeso.2014.11.017.

27. Jia-Tian Wong, Eng-Poh Ng, Farook Adam, Microscopic investigation of nanocrystalline zeolite L synthesized from rice husk ash, J. Am. Ceram. Soc. 95 (2012) 805–808. https://doi.org/10.1111/j.1551-2916.2011.04995.x.

28. I. Jiménez, G. Pérez, A. Guerrero, B. Ruiz, Mineral phases synthesized by hydrothermal treatment from biomass ashes, Int. J. Miner. Process. 158 (2017) 8-12. https://doi.org/10.1016/j.minpro.2016.11.002.

29. S. Vichaphund, D. Aht-Ong, V. Sricharoenchaikul, D. Atong, Characteristic of fly ash derived-zeolite and its catalytic performance for fast pyrolysis of Jatropha waste, Environ. Technol. 35 (2014) 2254-61. https://doi.org/10.1080/09593330.2014.900118.

30. T. Fukasawa, A. Horigome, T. Tsu, A.D. Karisma, N. Maeda, A.-N. Huang, K. Fukui, Utilization of incineration fly ash from biomass power plants for zeolite synthesis from coal fly ash by hydrothermal treatment, Fuel Process. Technol. 167 (2017) 92–98. https://doi.org/10.1016/j.fuproc.2017.06.023.

31. E.-P. Ng, J.-H. Chow, R.R. Mukti, O. Muraza, T.C. Ling, K.-L. Wong, Hydrothermal synthesis of zeolite A from bamboo leaf biomass and its catalytic activity in cyanoethylation of methanol under autogenic pressure and air conditions, Mater. Chem. Phys. 201 (2017) 78-85. https://doi.org/10.1016/j.matchemphys.2017.08.044.

32. K. Bunmai, N. Osakoo, K. Deekamwong, W. Rongchapo, C. Keawkumay, N. Chanlek, S. Prayoonpokarach, J. Wittayakun, Extraction of silica from cogon grass and utilization for synthesis of zeolite NaY by conventional and microwave-assisted hydrothermal methods, J. Taiwan Inst. Chem. E. 83 (2018) 152–158. https://doi.org/10.1016/j.jtice.2017.11.024.

33. V. P. Valtchev, K. N. Bozhilov, Transmission electron microscopy study of the formation of FAU-type zeolite at room temperature, J. Phys. Chem. B 108 (2004) 15587-15598. https://pubs.acs.org/doi/abs/10.1021/jp048341c.

34. A.M. Doyle, Z.T. Alismaeel, T.M. Albayati, A.S. Abbas, High purity FAU-type zeolite catalysts from shale rock for biodiesel production, Fuel 199 (2017) 394-402. https://doi.org/10.1016/j.fuel.2017.02.098.

35. M. Gross-Lorgouilloux, P. Caullet, M. Soulard, J. Patarin, E. Moleiro, I. Saude, Conversion of coal fly ashes into faujasite under soft temperature and pressure conditions. Mechanisms of crystallisation, Microporous and Mesoporous Materials 131 (2010) 407–417. https://doi.org/10.1016/j.micromeso.2010.01.022.

354 36. P. Kunecki, R. Panek, M. Wdowin, W. Franus, Synthesis of faujasite (FAU) and
355 tschernichite (LTA) type zeolites as a potential direction of the development of lime Class C
356 fly ash, Int. J. Miner. Process. 166 (2017) 69-78. https://doi.org/10.1016/j.minpro.2017.07.007.
357 37. R.M. Shayib, N.C. George, R. Seshadri, A.W. Burton, S.I. Zones, B. F. Chmelka, Structure-
358 directing roles and interactions of fluoride and organocations with siliceous zeolite
359 frameworks, J. Am. Chem. Soc. 133 (2011) 18728–18741. https://10.1021/ja205164u.
360 38. F. Fenglian, Q. Wang, Removal of heavy metal ions from wastewaters: A review, J.
361 Environ. Manage. 92 (2011) 407-418. https://doi.org/10.1016/j.jenvman.2010.11.011.